PHYSICAL REVIEW D **85,** 071102(R) (2012)

Search for double charmonium decays of the *P*-wave spin-triplet bottomonium states

C. P. Shen,[29] C. Z. Yuan,[12] T. Iijima,[30,29] I. Adachi,[9] H. Aihara,[52] K. Arinstein,[2] D. M. Asner,[40] T. Aushev,[16] A. M. Bakich,[46] B. Bhuyan,[10] M. Bischofberger,[31] A. Bozek,[35] M. Bračko,[26,17] T. E. Browder,[8] M.-C. Chang,[4] A. Chen,[32] B. G. Cheon,[7] K. Chilikin,[16] R. Chistov,[16] I.-S. Cho,[58] K. Cho,[20] S.-K. Choi,[6] Y. Choi,[45] J. Dalseno,[27,48] Z. Drásal,[3] A. Drutskoy,[16] S. Eidelman,[2] J. E. Fast,[40] V. Gaur,[47] N. Gabyshev,[2] A. Garmash,[2] Y. M. Goh,[7] J. Haba,[9] T. Hara,[9] K. Hayasaka,[30] H. Hayashii,[31] Y. Horii,[30] Y. Hoshi,[50] W.-S. Hou,[34] H. J. Hyun,[22] A. Ishikawa,[51] R. Itoh,[9] M. Iwabuchi,[58] T. Iwashita,[31] T. Julius,[28] J. H. Kang,[58] T. Kawasaki,[37] H. J. Kim,[22] H. O. Kim,[22] J. B. Kim,[21] K. T. Kim,[21] M. J. Kim,[22] Y. J. Kim,[20] B. R. Ko,[21] S. Koblitz,[27] P. Kodyš,[3] S. Korpar,[26,17] P. Križan,[24,17] P. Krokovny,[2] T. Kumita,[54] Y.-J. Kwon,[58] J. S. Lange,[5] S.-H. Lee,[21] J. Li,[44] J. Libby,[11] C.-L. Lim,[58] C. Liu,[43] Z. Q. Liu,[12] D. Liventsev,[16] R. Louvot,[23] S. McOnie,[46] K. Miyabayashi,[31] H. Miyata,[37] Y. Miyazaki,[29] R. Mizuk,[16] G. B. Mohanty,[47] A. Moll,[27,48] T. Mori,[29] N. Muramatsu,[42] R. Mussa,[15] E. Nakano,[39] M. Nakao,[9] H. Nakazawa,[32] S. Nishida,[9] K. Nishimura,[8] O. Nitoh,[55] S. Ogawa,[49] T. Ohshima,[29] S. Okuno,[18] S. L. Olsen,[44,8] Y. Onuki,[52] G. Pakhlova,[16] C. W. Park,[45] H. K. Park,[22] T. K. Pedlar,[25] M. Petrič,[17] L. E. Piilonen,[56] A. Poluektov,[2] M. Ritter,[27] M. Röhrken,[19] H. Sahoo,[8] Y. Sakai,[9] T. Sanuki,[51] Y. Sato,[51] O. Schneider,[23] C. Schwanda,[13] K. Senyo,[57] O. Seon,[29] M. Shapkin,[14] T.-A. Shibata,[53] J.-G. Shiu,[34] A. Sibidanov,[46] F. Simon,[27,48] J. B. Singh,[41] P. Smerkol,[17] Y.-S. Sohn,[58] E. Solovieva,[16] S. Stanič,[38] M. Starič,[17] T. Sumiyoshi,[54] G. Tatishvili,[40] Y. Teramoto,[39] T. Tsuboyama,[9] M. Uchida,[53] S. Uehara,[9] Y. Unno,[7] S. Uno,[9] P. Urquijo,[1] G. Varner,[8] K. E. Varvell,[46] C. H. Wang,[33] P. Wang,[12] X. L. Wang,[12] M. Watanabe,[37] Y. Watanabe,[18] E. Won,[21] Y. Yamashita,[36] Y. Yusa,[37] Z. P. Zhang,[43] V. Zhilich,[2] V. Zhulanov,[2] and A. Zupanc[19]

(Belle Collaboration)

[1]*University of Bonn, Bonn*
[2]*Budker Institute of Nuclear Physics SB RAS and Novosibirsk State University, Novosibirsk 630090*
[3]*Faculty of Mathematics and Physics, Charles University, Prague*
[4]*Department of Physics, Fu Jen Catholic University, Taipei*
[5]*Justus-Liebig-Universität Gießen, Gießen*
[6]*Gyeongsang National University, Chinju*
[7]*Hanyang University, Seoul*
[8]*University of Hawaii, Honolulu, Hawaii 96822*
[9]*High Energy Accelerator Research Organization (KEK), Tsukuba*
[10]*Indian Institute of Technology Guwahati, Guwahati*
[11]*Indian Institute of Technology Madras, Madras*
[12]*Institute of High Energy Physics, Chinese Academy of Sciences, Beijing*
[13]*Institute of High Energy Physics, Vienna*
[14]*Institute of High Energy Physics, Protvino*
[15]*INFN-Sezione di Torino, Torino*
[16]*Institute for Theoretical and Experimental Physics, Moscow*
[17]*J. Stefan Institute, Ljubljana*
[18]*Kanagawa University, Yokohama*
[19]*Institut für Experimentelle Kernphysik, Karlsruher Institut für Technologie, Karlsruhe*
[20]*Korea Institute of Science and Technology Information, Daejeon*
[21]*Korea University, Seoul*
[22]*Kyungpook National University, Taegu*
[23]*École Polytechnique Fédérale de Lausanne (EPFL), Lausanne*
[24]*Faculty of Mathematics and Physics, University of Ljubljana, Ljubljana*
[25]*Luther College, Decorah, Iowa 52101*
[26]*University of Maribor, Maribor*
[27]*Max-Planck-Institut für Physik, München*
[28]*University of Melbourne, School of Physics, Victoria 3010*
[29]*Graduate School of Science, Nagoya University, Nagoya*
[30]*Kobayashi-Maskawa Institute, Nagoya University, Nagoya*
[31]*Nara Women's University, Nara*
[32]*National Central University, Chung-li*
[33]*National United University, Miao Li*
[34]*Department of Physics, National Taiwan University, Taipei*
[35]*H. Niewodniczanski Institute of Nuclear Physics, Krakow*

[36]*Nippon Dental University, Niigata*
[37]*Niigata University, Niigata*
[38]*University of Nova Gorica, Nova Gorica*
[39]*Osaka City University, Osaka*
[40]*Pacific Northwest National Laboratory, Richland, Washington 99352*
[41]*Panjab University, Chandigarh*
[42]*Research Center for Nuclear Physics, Osaka University, Osaka*
[43]*University of Science and Technology of China, Hefei*
[44]*Seoul National University, Seoul*
[45]*Sungkyunkwan University, Suwon*
[46]*School of Physics, University of Sydney, NSW 2006*
[47]*Tata Institute of Fundamental Research, Mumbai*
[48]*Excellence Cluster Universe, Technische Universität München, Garching*
[49]*Toho University, Funabashi*
[50]*Tohoku Gakuin University, Tagajo*
[51]*Tohoku University, Sendai*
[52]*Department of Physics, University of Tokyo, Tokyo*
[53]*Tokyo Institute of Technology, Tokyo*
[54]*Tokyo Metropolitan University, Tokyo*
[55]*Tokyo University of Agriculture and Technology, Tokyo*
[56]*CNP, Virginia Polytechnic Institute and State University, Blacksburg, Virginia 24061*
[57]*Yamagata University, Yamagata*
[58]*Yonsei University, Seoul*

(Received 1 March 2012; published 18 April 2012)

Using a sample of 158×10^6 $\Upsilon(2S)$ events collected with the Belle detector, we search for the first time for double-charmonium decays of the P-wave spin-triplet bottomonium states ($\Upsilon(2S) \to \gamma\chi_{bJ}$, $\chi_{bJ} \to J/\psi J/\psi$, $J/\psi\psi'$, $\psi'\psi'$ for $J = 0$, 1, and 2). No significant χ_{bJ} signal is observed in the double-charmonium mass spectra, and we obtain the following upper limits: $\mathcal{B}(\chi_{bJ} \to J/\psi J/\psi) < 7.1 \times 10^{-5}$, 2.7×10^{-5}, 4.5×10^{-5}, $\mathcal{B}(\chi_{bJ} \to J/\psi\psi') < 1.2 \times 10^{-4}$, 1.7×10^{-5}, 4.9×10^{-5}, $\mathcal{B}(\chi_{bJ} \to \psi'\psi') < 3.1 \times 10^{-5}$, 6.2×10^{-5}, 1.6×10^{-5} for $J = 0$, 1, and 2, respectively, at the 90% confidence level. These limits are significantly lower than the central values (with uncertainties of 50% to 70%) predicted using the light cone formalism but are consistent with calculations using the nonrelativistic QCD (NRQCD) factorization approach.

DOI: 10.1103/PhysRevD.85.071102 PACS numbers: 13.25.Gv, 13.25.Hw, 14.40.Pq

The order of magnitude discrepancy between the cross-sections of the double-charmonium production processes $e^+e^- \to J/\psi\eta_c$, $J/\psi\eta_c'$, $\psi'\eta_c$, $\psi'\eta_c'$, $J/\psi\chi_{c0}$, and $\psi'\chi_{c0}$ measured in the Belle [1,2] and *BABAR* [3] experiments and those of the leading-order nonrelativistic QCD predictions [4–6] has been a great challenge to theorists. After great efforts, it was shown that agreement can be achieved by taking into account QCD radiative and relativistic corrections [4,7–10].

As in e^+e^- annihilation, double-charmonium final states can also be formed in bottomonium decays, which provide a new test of the dynamics of hard exclusive processes and charmonium structure. While the rate of $\eta_b \to J/\psi J/\psi$ decay was calculated some time ago by many authors [11], the rates for P-wave spin-triplet bottomonium states χ_{bJ} ($J = 0$, 1, 2) decays into double-charmonium states were calculated only recently using various theoretical models after a first attempt about 30 years ago with a perturbative QCD method [12].

The authors of Ref. [13] calculated $\chi_{bJ} \to J/\psi J/\psi$ in the framework of the NRQCD factorization formalism, including second-order relativistic corrections in the relative charm-quark velocity v_c, as well as an electromagnetic correction. The branching fraction is predicted to be of order 10^{-5} for χ_{b0} or $\chi_{b2} \to J/\psi J/\psi$, and 10^{-11} for $\chi_{b1} \to J/\psi J/\psi$. The authors of Ref. [14] considered corrections to all orders in v_c in the charmonium rest frame and found decay partial widths that are about a factor of 3 larger than those in Ref. [13]. In the light cone formalism, however, much larger production rates (with uncertainties of 50% to 70%) are obtained in Ref. [15]: $\mathcal{B}(\chi_{bJ} \to J/\psi J/\psi) = 9.6 \times 10^{-5}$ or 1.1×10^{-3}, $\mathcal{B}(\chi_{bJ} \to J/\psi\psi') = 1.6 \times 10^{-4}$ or 1.6×10^{-3}, and $\mathcal{B}(\chi_{bJ} \to \psi'\psi') = 6.6 \times 10^{-5}$ or 5.9×10^{-4} for $J = 0$ or 2, respectively. These results are not very different from the perturbative QCD calculation with the relative motion of the charm-quark in the χ_b decays taken into account [16]. It is therefore necessary to pin down the source of such a significant difference among various models.

In this paper, we report a search for χ_{bJ} decays to double-charmonium in $\Upsilon(2S)$ radiative transitions, i.e.,

$\Upsilon(2S) \to \gamma\chi_{bJ} \to \gamma J/\psi J/\psi$, $\gamma J/\psi\psi'$, and $\gamma\psi'\psi'$. In order to detect the signal efficiently, we require only one J/ψ or ψ' candidate to be fully reconstructed (or "tagged"). We require that the missing mass of the J/ψ (or ψ') and the radiative photon candidate be in the J/ψ or ψ' mass region. The missing mass is defined as $M_{\rm miss} = \sqrt{(P_{e^+e^-} - P_f)^2}$, where $P_{e^+e^-}$ is the 4-momentum of the e^+e^- collision system and P_f is the sum of the 4-momentum of the observed final-state particles. Double counting of an event is allowed if both charmonium states satisfy the tag criteria. The probability of double counting depends on the final states and varies from a few per mille to less than 5%; this is taken into account in the efficiency estimation using Monte Carlo (MC) samples generated with both charmonium states decaying generically. For $\gamma J/\psi J/\psi$, we reconstruct one J/ψ signal from $\ell^+\ell^-$ ($\ell = e$ or μ) and require the missing mass of $\gamma J/\psi$ be within the J/ψ mass region. For $\gamma J/\psi\psi'$, three modes are included: (1) $J/\psi \to \ell^+\ell^-$ with $M_{\rm miss}(\gamma J/\psi)$ required to be within the ψ' mass region; (2) $\psi' \to \pi^+\pi^- J/\psi \to \pi^+\pi^-\ell^+\ell^-$ with $M_{\rm miss}(\gamma\psi')$within the J/ψ mass region; (3) $\psi' \to \ell^+\ell^-$ with $M_{\rm miss}(\gamma\psi')$ within the J/ψ mass region. For $\gamma\psi'\psi'$, two modes are used: (1) one $\psi' \to \pi^+\pi^- J/\psi \to \pi^+\pi^-\ell^+\ell^-$ is identified and $M_{\rm miss}(\gamma\psi')$ is required to be within the ψ' mass region; (2) one $\psi' \to \ell^+\ell^-$ is identified and $M_{\rm miss}(\gamma\psi')$ is required to be within the ψ' mass region.

This analysis is based on a 24.7 fb^{-1} $\Upsilon(2S)$ data sample (158×10^6 $\Upsilon(2S)$ events [17]), and a 89.4 fb^{-1} continuum data sample collected at $\sqrt{s} = 10.52$ GeV. Here $\sqrt{s}$ is the center-of-mass (CM) energy of the colliding e^+e^-. The data are collected with the Belle detector [18] operating at the KEKB asymmetric-energy e^+e^- collider [19].

EVTGEN [20] was used to generate MC simulation events. For signal MC samples, the angular distribution for $\Upsilon(2S) \to \gamma\chi_{bJ}$ is simulated assuming a pure E1 transition ($dN/d\cos\theta_\gamma \propto 1 + \alpha\cos^2\theta_\gamma$, $\alpha = 1, -\frac{1}{3}, \frac{1}{13}$ for $J = 0, 1, 2$, respectively [21]). Here θ_γ is the polar angle of the $\Upsilon(2S)$ radiative photon in the e^+e^- CM frame. Uniform phase space is used for χ_{bJ} decays [22].

Since no experimental measurements are available for the widths of χ_{bJ} [23], and the theoretical expectations are at 1 MeV level or less [13], the widths of χ_{bJ} are set to be zero. Generic decay modes are used for the J/ψ and ψ'. $\Upsilon(2S)$ MC events with generic decays produced with PYTHIA [24] with 2 times the effective luminosity of data are used to check the possible backgrounds from $\Upsilon(2S)$ decays.

The detector is described in detail elsewhere [18]. It is a large-solid-angle magnetic spectrometer that consists of a silicon vertex detector, a 50-layer central drift chamber (CDC), an array of aerogel threshold Cherenkov counters, a barrel-like arrangement of time-of-flight scintillation counters, and an electromagnetic calorimeter (ECL) comprised of CsI(T1) crystals located inside a superconducting solenoid coil that provides a 1.5 T magnetic field. An iron flux-return located outside the coil is instrumented to detect K_L^0-mesons and to identify muons.

For well-reconstructed charged tracks, the impact parameters perpendicular to and along the beam direction with respect to the nominal interaction point are required to be less than 0.5 cm and 4 cm, respectively, and the transverse momentum in the laboratory frame is required to be larger than 0.1 GeV/c. We require the number of well-reconstructed charged tracks to be greater than 3 for $\gamma J/\psi J/\psi$ and greater than 4 for $\gamma J/\psi\psi'$ and $\gamma\psi'\psi'$. For the modes with ψ' in the final states, events with exactly 4 charged tracks are removed to suppress the significant background from QED processes. For each charged track, information from different detector subsystems is combined to form a likelihood $\mathcal{L}_i$ for each particle species [25]. A track with $\mathcal{R}_K = \frac{\mathcal{L}_K}{\mathcal{L}_K + \mathcal{L}_\pi} < 0.4$ is identified as a pion with an efficiency of about 97% for the momentum range of interest; about 3.5% are misidentified K tracks. For electron identification, the likelihood ratio is defined as $\mathcal{R}_e = \frac{\mathcal{L}_e}{\mathcal{L}_e + \mathcal{L}_x}$, where $\mathcal{L}_e$ and $\mathcal{L}_x$ are the likelihoods for electron and nonelectron, respectively, determined using the ratio of the energy deposit in the ECL to the momentum measured in the SVD and CDC, the shower shape in the ECL, matching between the position of the charged track trajectory and the cluster position in the ECL, the hit information from the aerogel threshold Cherenkov counter, and the dE/dx information in the CDC [26]. For muon identification, the likelihood ratio is defined as $\mathcal{R}_\mu = \frac{\mathcal{L}_\mu}{\mathcal{L}_\mu + \mathcal{L}_\pi + \mathcal{L}_K}$, where $\mathcal{L}_\mu$, $\mathcal{L}_\pi$, and $\mathcal{L}_K$ are the likelihoods for muon, pion, and kaon hypotheses, respectively, based on the matching quality and penetration depth of associated hits in the K_L^0-meson [27].

A neutral cluster is used as a photon candidate if it does not match the extrapolation of any charged track and its energy is greater than 50 MeV. In calculating the recoil mass of $\gamma J/\psi$ or $\gamma\psi'$, all photon candidates except those within 0.05 radians of the electron/positron tracks are included. No π^0 signal is observed in combining the low-energy radiative photon with any of the remaining photon candidates in the event after all the selection criteria are applied.

In order to correct for the effect of bremsstrahlung and final-state radiation, photons detected in the ECL within 0.05 radians of the original e^+ or e^- direction are included in the calculation of the e^+/e^- momentum. For the lepton pair used to reconstruct J/ψ, both tracks should have $\mathcal{R}_e > 0.95$ in the e^+e^- mode, or one track should have $\mathcal{R}_\mu > 0.95$ while the other should satisfy $\mathcal{R}_\mu > 0.05$ in the $\mu^+\mu^-$ mode. The lepton pair identification efficiency is about 90% for $J/\psi \to e^+e^-$ and 87% for $J/\psi \to \mu^+\mu^-$. In order to improve the J/ψ momentum

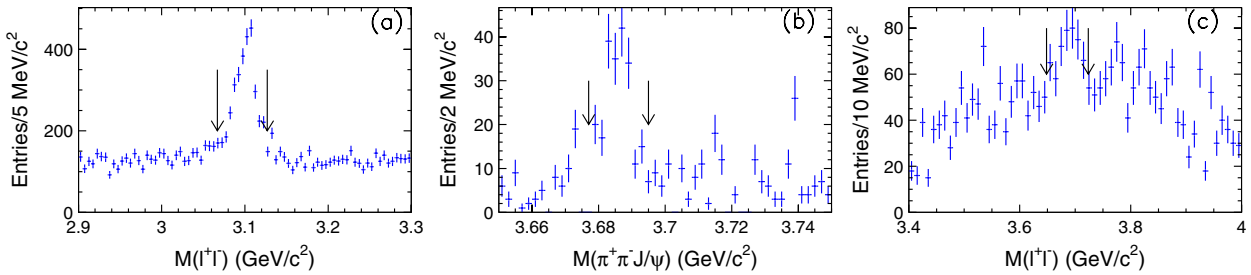

FIG. 1 (color online). The reconstructed (a) $J/\psi \to \ell^+\ell^-$, (b) $\psi' \to \pi^+\pi^- J/\psi$, and (c) $\psi' \to \ell^+\ell^-$ candidates mass distributions from data. The arrows show the required signal mass regions.

resolution, a mass-constrained fit is then performed for J/ψ signals in all the modes. As different modes have almost the same J/ψ mass resolutions, the J/ψ signal region is defined as $|M_{\ell^+\ell^-} - m_{J/\psi}| < 0.03$ GeV/c^2 ($\approx 2.5\sigma$), where $m_{J/\psi}$ is the nominal mass of J/ψ [23]. The J/ψ mass sidebands are defined as 2.97 GeV/c^2 < $M_{\ell^+\ell^-}$ < 3.03 GeV/c^2 or 3.17 GeV/c^2 < $M_{\ell^+\ell^-}$ < 3.23 GeV/c^2, and are twice as wide as the signal region. For $\psi' \to \ell^+\ell^-$, the ψ' signal region is defined as $|M_{\ell^+\ell^-} - m_{\psi'}| < 0.0375$ GeV/c^2 ($\approx 2.5\sigma$), where $m_{\psi'}$ is the nominal mass of ψ' [23]. The ψ' mass sidebands are defined as 3.535 GeV/c^2 < $M_{\ell^+\ell^-}$ < 3.610 GeV/c^2 or 3.760 GeV/c^2 < $M_{\ell^+\ell^-}$ < 3.835 GeV/c^2 and are twice as wide as the signal region. For $\psi' \to \pi^+\pi^- J/\psi$, we require the two pion candidates be positively identified. The ψ' signal region is defined as $|M_{\pi^+\pi^- J/\psi} - m_{\psi'}| <$ 0.009 GeV/c^2 ($\approx 3\sigma$). Figure 1 shows (a) the mass distributions of the reconstructed $J/\psi \to \ell^+\ell^-$, (b) $\psi' \to \pi^+\pi^- J/\psi$, and (c) $\psi' \to \ell^+\ell^-$ candidates.

Figure 2 shows scatter plots of the photon spectra in the e^+e^- CM frame versus (a) $M_{\rm miss}(\gamma J/\psi)$ with $J/\psi \to \ell^+\ell^-$ reconstructed, (b) $M_{\rm miss}(\gamma\psi')$ with $\psi' \to \pi^+\pi^- J/\psi$ reconstructed, and (c) $M_{\rm miss}(\gamma\psi')$ with $\psi' \to \ell^+\ell^-$ reconstructed. No evidence for J/ψ or ψ' signals can be seen in the $\gamma J/\psi$ or $\gamma\psi'$ missing mass distributions.

Figure 3 shows the simulated photon spectra in the e^+e^- CM frame from the $\Upsilon(2S) \to \gamma\chi_{bJ} \to \gamma J/\psi J/\psi$ MC samples. Breit-Wigner functions convolved with Novosibirsk functions [28] are used as χ_{bJ} signal shapes while Chebychev polynomial functions model the combinatorial backgrounds ($\sim 11\%$ in χ_{bJ} signal region). The extended maximum likelihood fits to the photon spectra with all the parameters free are shown in Fig. 3. Based on the fit results, the efficiencies are $(5.75 \pm 0.12)\%$, $(6.25 \pm 0.12)\%$, and $(5.87 \pm 0.12)\%$ for $\Upsilon(2S) \to \gamma\chi_{bJ} \to \gamma J/\psi J/\psi$ for $J = 0$, 1 and 2, respectively. Similarly, the sum of the efficiencies from all the modes is found to be $(3.40 \pm 0.06)\%$, $(3.78 \pm 0.06)\%$, and $(3.53 \pm 0.06)\%$ for $\Upsilon(2S) \to \gamma\chi_{bJ} \to \gamma J/\psi\psi'$, $(2.06 \pm 0.04)\%$, $(2.15 \pm 0.04)\%$, and $(2.09 \pm 0.04)\%$ for $\Upsilon(2S) \to \gamma\chi_{bJ} \to \gamma\psi'\psi'$ for $J = 0$, 1 and 2, respectively.

After all the event selections, no events from the $\Upsilon(2S)$ MC sample with generic decays survive. Other possible backgrounds with $J/\psi/\psi'$ signals from channels such as $e^+e^- \to J/\psi\chi_{cJ}$, $\psi'\chi_{cJ}$, have very small cross-sections (at the few fb level [29]) and hence are neglected in the analysis.

Figs. 4(a)–4(c) show the photon spectra from $\Upsilon(2S)$ data for $\chi_{bJ} \to J/\psi J/\psi$, $J/\psi\psi'$, and $\psi'\psi'$ candidate events, respectively, with all the modes included. Here the shaded histograms show the J/ψ or ψ' mass sidebands normalized to the width of the J/ψ or ψ' signal range, and the dashed histograms are the normalized continuum contributions. The continuum background contribution is extrapolated down to the $\Upsilon(2S)$ resonance. For the extrapolation, three factors are applied to account for: the relative luminosities of the two samples, efficiency dependence on

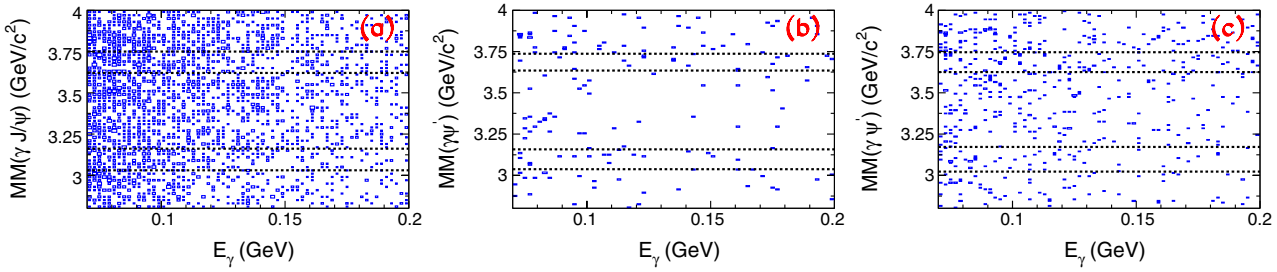

FIG. 2 (color online). Scatter plots of the photon spectra in the e^+e^- CM frame versus (a) $M_{\rm miss}(\gamma J/\psi)$ with $J/\psi \to \ell^+\ell^-$ reconstructed, (b) $M_{\rm miss}(\gamma\psi')$ with $\psi' \to \pi^+\pi^- J/\psi$ reconstructed, and (c) $M_{\rm miss}(\gamma\psi')$ with $\psi' \to \ell^+\ell^-$ reconstructed. The dotted lines show the J/ψ or ψ' signal regions ($\approx \pm 3\sigma$).

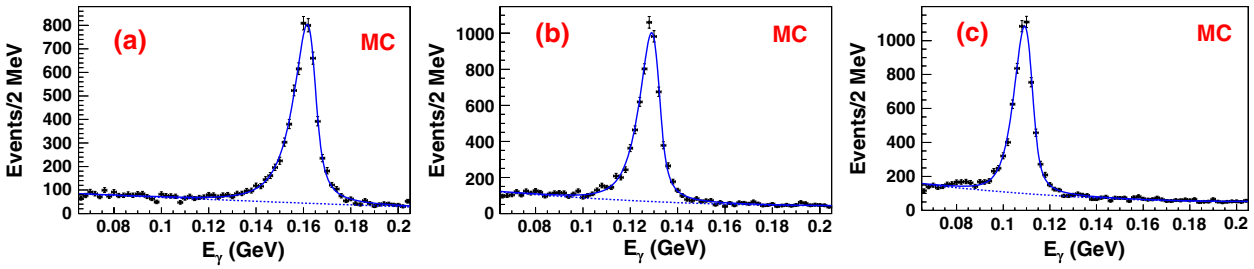

FIG. 3 (color online). The fits to the photon spectra from the $\Upsilon(2S) \to \gamma\chi_{bJ} \to \gamma J/\psi J/\psi$ MC signal samples with one J/ψ reconstructed and the $\gamma J/\psi$ recoil mass within the J/ψ mass region for (a) χ_{b0}, (b) χ_{b1}, and (c) χ_{b2}, respectively. The χ_{bJ} shapes are described by Breit-Wigners convolved with Novosibirsk functions, while Chebychev polynomial functions are used to describe the background.

the CM energy, and cross-section dependence on the CM energy. The cross-section extrapolation with CM energy is assumed to have a $1/s$ dependence.

No clear χ_{bJ} signals are observed in Fig. 4. For $\chi_{bJ} \to J/\psi J/\psi$, an unbinned extended maximum likelihood method is applied to the photon spectrum with the MC simulated signal shape smeared with a Gaussian function to take into account a 8.5% difference in photon energy resolution between data and MC samples. The photon energy resolution is measured with $\Upsilon(2S) \to \gamma\chi_{bJ} \to \gamma\gamma\Upsilon(1S)$, $\Upsilon(1S) \to \mu^+\mu^-$ events. For $\chi_{bJ} \to J/\psi\psi'$ ($\psi'\psi'$) decays, an unbinned extended maximum likelihood simultaneous fit is performed to all the modes mentioned above. The ratios of the χ_{bJ} yields in different modes are fixed to ε_i (i denotes the ith mode) with all the intermediate state branching fractions included, and ε_i is the MC-determined efficiency for the ith mode. The fits are performed with the same method as in the $J/\psi J/\psi$ mode. Figure 4 shows the fit results, where for (b) and (c) the solid curves are the sum of all the fit contributions and the dashed curves are the sum of the background functions. In all of the modes, the background levels from the fits are a little higher than the estimations from the normalized continuum or the normalized $J/\psi/\psi'$ mass sidebands. It may indicate that there are double-charmonium productions together with one photon or more particles in $\Upsilon(2S)$ decays.

The upper limit on the number of signal events at the 90% C.L. ($n^{\rm up}$) is calculated by solving the equation $\frac{\int_0^{n^{\rm up}} \mathcal{L}(x)dx}{\int_0^{+\infty} \mathcal{L}(x)dx} = 0.9$, where x is the number of signal events and $\mathcal{L}(x)$ is the likelihood function depending on x from the fit to the data, with x being the number of signal events in the fit. The values of $n^{\rm up}$ are found to be 21, 13, and 22 for $\chi_{bJ} \to J/\psi J/\psi$; 20, 5.8, and 17 for $\chi_{bJ} \to J/\psi\psi'$; and 3.0, 12, and 3.3 for $\chi_{bJ} \to \psi'\psi'$, for $J = 0$, 1, and 2, respectively, when requiring the signal yields to be non-negative in the fit.

There are several sources of systematic errors for the branching fraction measurement. The uncertainty in the

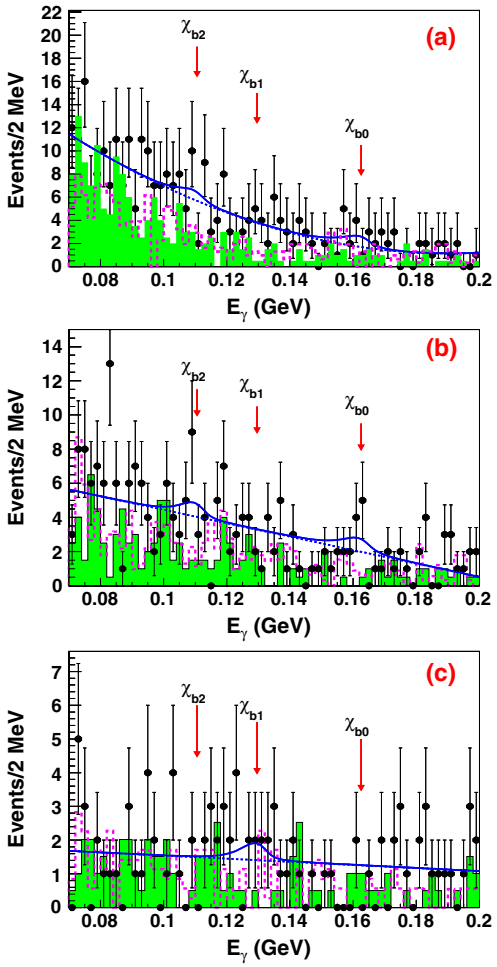

FIG. 4 (color online). The photon spectra in $\Upsilon(2S)$ data for (a) $\gamma J/\psi J/\psi$, (b) $\gamma J/\psi\psi'$, and (c) $\gamma\psi'\psi'$ final states. The shaded histograms are from normalized $J/\psi/\psi'$ mass sidebands events, and dashed histograms are normalized continuum contributions. The fits to the photon spectra are described in the text. The solid curves are the best fits; the dashed curves represent the backgrounds. The arrows show the expected central positions of the χ_{bJ} states.

TABLE I. Summary of the limits on χ_{bJ} decays into $J/\psi J/\psi$, $J/\psi\psi'$, and $\psi'\psi'$. Here $n^{\rm up}$ is the upper limit on the number of signal events, ε is the sum of the efficiencies from different modes with J/ψ and ψ' decay branching fractions and trigger efficiency included, $\sigma_{\rm sys}$ is the total systematic error, and $\mathcal{B}_R$ is the upper limit on the branching fraction of χ_{bJ} decays, where the values of $\mathcal{B}(\Upsilon(2S) \to \gamma\chi_{bJ}) = (3.8 \pm 0.4)\%$, $(6.9 \pm 0.4)\%$, and $(7.15 \pm 0.35)\%$ for $J = 0$, 1, and 2 are used [23]. The upper limits are at 90% C.L.

Channel	$n^{\rm up}$	$\varepsilon(\%)$	$\sigma_{\rm sys}(\%)$	$\mathcal{B}_R$
$\chi_{b0} \to J/\psi J/\psi$	21	5.8	16	7.1×10^{-5}
$\chi_{b1} \to J/\psi J/\psi$	13	6.3	30	2.7×10^{-5}
$\chi_{b2} \to J/\psi J/\psi$	22	5.9	27	4.5×10^{-5}
$\chi_{b0} \to J/\psi\psi'$	20	3.4	17	1.2×10^{-4}
$\chi_{b1} \to J/\psi\psi'$	5.8	3.8	15	1.7×10^{-5}
$\chi_{b2} \to J/\psi\psi'$	17	3.5	16	4.9×10^{-5}
$\chi_{b0} \to \psi'\psi'$	3.0	2.1	20	3.1×10^{-5}
$\chi_{b1} \to \psi'\psi'$	12	2.2	17	6.2×10^{-5}
$\chi_{b2} \to \psi'\psi'$	3.3	2.1	12	1.6×10^{-5}

tracking efficiency for tracks with angles and momenta characteristic of signal events is about 0.35% per track and is additive. The photon reconstruction contributes an additional 3.8% per photon. The uncertainty due to particle identification efficiency is 1.3% for each pion in $\psi' \to \pi^+\pi^- J/\psi$. According to a measurement of the lepton identification efficiency using a control sample of $\gamma\gamma \to \ell^+\ell^-$, the MC simulates data within 1.7% for an electron-positron pair and 1.7% for a muon pair. According to MC simulation, the trigger efficiency is greater than 99.5% and we take 0.5% as systematic error due to the trigger simulation uncertainty. Errors on the branching fractions of the intermediate states are taken from the Particle Data Group [23], which are about 12%, 6.0%, and 5.0% for χ_{b0}, χ_{b1}, and χ_{b2} decays, respectively. By changing the order of the background polynomial and the range of the fit, the relative difference in the upper limits of the number of signal events is 7.6%–28% depending on the decay mode, which is taken as systematic error due to the uncertainty of fit. For our MC signal samples, J/ψ and ψ' decays are simulated with a generic decay model. The signal efficiencies are determined based on the fitted results. The error on the number of fitted signal events is less than 2.1%, which is taken as the MC statistical error in the efficiency. The masses of χ_{bJ} have been measured well [23] and the uncertainties on the masses of χ_{bJ} do not affect the efficiency determination. Comparing several theoretical calculations, the maximum values of χ_{b0} and χ_{b2} widths are 2.15 MeV/c^2 [30] and 0.33 MeV/c^2 [31], respectively. The efficiency differences between these values and the nominal values are taken as systematic errors due to the uncertainty of resonance parameters, which are less than 5.2% and 1.2% for χ_{c0} and χ_{b2} decays. Finally, the uncertainty on the total number of $\Upsilon(2S)$ events is 2.3%. Assuming that all of these systematic error sources are independent, and combining them in quadrature, we obtain the total systematic error listed in Table I.

Since there is no evidence for signals in the modes studied, we determine upper limits on the branching fractions of χ_{bJ} to double charmonia. Table I lists the upper limits $n^{\rm up}$ for the numbers of the signal events, detection efficiencies, systematic errors, and upper limits on the branching fractions of χ_{bJ} decays. In order to calculate conservative upper limits on these branching fractions, the efficiencies are lowered by a factor of $1 - \sigma_{\rm sys}$ in the calculation.

To summarize, we find no significant signals in the $\chi_{bJ} \to J/\psi J/\psi$, $J/\psi\psi'$, or $\psi'\psi'$ final states using a sample of 158×10^6 $\Upsilon(2S)$ events. The results obtained on the χ_{bJ} decay branching fractions are listed in Table I. Our upper limits are much lower than the central values predicted in the light cone formalism [15] and pQCD calculation [16], but are consistent with calculations using the NRQCD factorization approach [13,14].

We thank the KEKB group for excellent operation of the accelerator, the High Energy Accelerator Research Organization (KEK) cryogenics group for efficient solenoid operations, the KEK computer group and National Institute of Informatics for valuable computing and SINET4 network support. We acknowledge support from MEXT, JSPS, and Nagoya's TLPRC (Japan); ARC and DIISR (Australia); NSFC (China); MSMT(Czech Republic); DST(India); MEST, NRF, NSDC of KISTI, and WCU(Korea); MNiSW(Poland); MESand RFAAE (Russia); ARRS (Slovenia); SNSF (Switzerland); NSC and MOE (Taiwan); and DOE and NSF (USA).

[1] K. Abe *et al.* (Belle Collaboration), Phys. Rev. Lett. **89**, 142001 (2002).
[2] K. Abe *et al.* (Belle Collaboration), Phys. Rev. D **70**, 071102 (2004).
[3] B. Aubert *et al.* (*BABAR* Collaboration), Phys. Rev. D **72**, 031101 (2005).
[4] E. Braaten and J. Lee, Phys. Rev. D **67**, 054007 (2003).
[5] K. Y. Liu, Z. G. He, and K. T. Chao, Phys. Lett. B **557**, 45 (2003).
[6] K. Y. Liu, Z. G. He, and K. T. Chao, Phys. Rev. D **77**, 014002 (2008).

[7] G. T. Bodwin, J. Lee, and E. Braaten, Phys. Rev. Lett. **90**, 162001 (2003).
[8] Y. J. Zhang, Y. J. Gao, and K. T. Chao, Phys. Rev. Lett. **96**, 092001 (2006).
[9] G. T. Bodwin, J. Lee, and C. Yu, Phys. Rev. D **77**, 094018 (2008).
[10] Z. G. He, Y. Fan, and K. T. Chao, Phys. Rev. D **75**, 074011 (2007).
[11] P. Sun, G. Hao, and C. F. Qiao, Phys. Lett. B **702**, 49 (2011) and references therein.
[12] V. G. Kartvelishvili and A. K. Likhoded, Yad. Fiz. **40**, 1273 (1984).
[13] J. Zhang, H. R. Dong, and F. Feng, Phys. Rev. D **84**, 094031 (2011).
[14] W. L. Sang, R. Rashidin, U. Kim, and J. Lee, Phys. Rev. D **84**, 074026 (2011).
[15] V. V. Braguta, A. K. Likhoded, and A. V. Luchinsky, Phys. Rev. D **80**, 094008 (2009); Phys. At. Nucl. **73**, 1054 (2010).
[16] V. V. Braguta, A. K. Likhoded, and A. V. Luchinsky, Phys. Rev. D **72**, 094018 (2005).
[17] X. L. Wang *et al.* (Belle Collaboration), Phys. Rev. D **84**, 071107(R) (2011).
[18] A. Abashian *et al.* (Belle Collaboration), Nucl. Instrum. Methods Phys. Res., Sect. A **479**, 117 (2002).
[19] S. Kurokawa and E. Kikutani, Nucl. Instrum. Methods Phys. Res., Sect. A **499**, 1 (2003), and other papers included in this volume.
[20] D. J. Lange, Nucl. Instrum. Methods Phys. Res., Sect. A **462**, 152 (2001).
[21] K. W. Edwards *et al.* (CLEO Collaboration), Phys. Rev. D **59**, 032003 (1999).
[22] For χ_{bJ} decays, MC signal samples are also produced with the helicity amplitude formulae from $\chi_{cJ} \to VV$ ($V = \omega$ or ϕ) [32] or from Ref. [13]. The largest difference in the efficiencies is less than 10%. The efficiencies with the phase space mode are lower, which will give conservative upper limits on the production rates.
[23] K. Nakamura *et al.* (Particle Data Group), J. Phys. G **37**, 075021 (2010) and 2011 partial update for the 2012 edition.
[24] T. Sjostrand, S. Mrenna, and P. Skands, J. High Energy Phys. 05 (2006) 026.
[25] E. Nakano, Nucl. Instrum. Methods Phys. Res., Sect. A **494**, 402 (2002).
[26] K. Hanagaki *et al.*, Nucl. Instrum. Methods Phys. Res., Sect. A **485**, 490 (2002).
[27] A. Abashian, K. Abe, K. Abe, P. K. Behera, F. Handa, T. Iijima, Y. Inoue, H. Miyake, T. Nagamine, E. Nakano, S. Narita, L. Piilonen, S. Schrenk, Y. Teramoto, K. Trabelsi, J. G. Wang, M. Yamaga, A. Yamaguchi, Y. Yusa, Nucl. Instrum. Methods Phys. Res., Sect. A **491**, 69 (2002).
[28] The Novosibirsk function is defined as $f(x) = \exp[-\frac{1}{2}(\ln^2(1 + \Lambda(x - x_0))/\tau^2 + \tau^2)]$, with $\Lambda = \sinh(\tau\sqrt{\ln 4})/(\sigma\sqrt{\ln 4})$. The parameters represent the mean (x_0), the width (σ), and the tail asymmetry (τ).
[29] K. Wang, Y. Q. Ma, and K. T. Chao, Phys. Rev. D **84**, 034022 (2011).
[30] S. N. Gupta, J. M. Johnson, and W. W. Repko, Phys. Rev. D **54**, 2075 (1996).
[31] J. T. Laverty, S. F. Radford, and W. W. Repko, arXiv:0901.3917.
[32] M. Ablikim *et al.* (BESIII Collaboration), Phys. Rev. Lett. **107**, 092001 (2011).